

Pre-fracture zone model on magnetoelectrically permeable interface crack between two dissimilar magnetoelastoelectroelastic materials

Peng MA¹, Wenjie Feng^{2,*}, Ray Kai Leung Su¹

¹ Department of Civil Engineering, The University of Hong Kong, PR China

² Department of Engineering Mechanics, Shijiazhuang Tiedao University, Shijiazhuang 050043, PR China

* Corresponding author: wjfeng9999@yahoo.com (W.J. Feng)

Abstract A plane strain problem for two magnetoelastoelectroelastic (MEE) half-planes adhered by a thin isotropic interlayer is considered. A novel crack model, i.e., a magnetoelectrically permeable interface crack with pre-fracture zones is introduced for MEE bimaterial system. The stresses in pre-fracture zones and the lengths of pre-fracture zones are unknown, which are determined by solving the corresponding Hilbert problem and solving nonlinear equations introduced by yielding condition on the pre-fracture zones. Some particular cases are further analyzed and numerically discussed. In the suggested model, any singularities connected with the crack are eliminated, and the results presented in this paper should have potential applications to the design of multilayered MEE structures and devices.

Keywords Pre-fracture zone, Interface crack, Magnetoelectrically permeable, Magnetoelastoelectroelastic plane

1. Introduction

Magnetoelastoelectroelastic (MEE) materials have been widely used in electronics industry. In the design of MEE structures, it is important to take into account the defects/imperfections, such as cracks, which are often pre-existing or are generated by external loads during the service life. Therefore, in recent years, research on fracture mechanics of MEE materials has drawn a lot of interest, and lots of achievements have been made for two-dimensional (2-D) internal crack problems [1-5] and 2-D interface crack problems [6-8]. It is noted that in the works of [7] and [8], the contact zone model is firstly extended to interface crack problems of MEE materials.

However, all the above-mentioned works related to interface crack problems, the singularity behavior on the crack tips always exists. On the other hand, two kinds of MEE materials, as well known, generally cannot be connected directly. Thus, in this study, a novel interface crack model for MEE bimaterial, i.e., the model of interface crack with pre-fracture zones is put forward. For simplicity, the interface is assumed to be magnetoelectrically permeable. The problem is reduced to solve a Hilbert problem and two nonlinear equations introduced by Mises yielding condition. The particular cases of symmetric loads and identical MEE material are further analyzed, and some numerical results are presented. These obtained results and/or conclusions could be of interest to the analysis and design of smart sensors/actuators constructed from MEE composite laminates.

2. Statement of the problem

Referring to Ref. [9], it is assumed that the MEE half-spaces are adhered by means of an isotropic interlayer with shear modulus μ , Poisson's ratio ν and yield limit σ_Y . Furthermore, the half-spaces are assumed to be loaded at infinity with uniform stresses $\sigma_{33}^{(m)} = \sigma_0$, $\sigma_{31}^{(m)} = \tau_0$, uniform electrical displacement $D_3^{(m)} = d_0$ and magnetic induction $B_3^{(m)} = b_0$ ($m=1$ stands for the upper domain, and $m=2$ for the lower one). In this paper, although the interlayer thickness will not be taken into account as usual, the properties of the interlayer and its influence upon the fracture process will be considered by means of introduction of pre-fracture zones with cohesive stresses. As shown in Fig. 1, the pre-fracture zones are, respectively, denoted by $[a_1, a]$ and $[b, b_1]$, and the

open part of the crack is denoted by $[a, b]$.

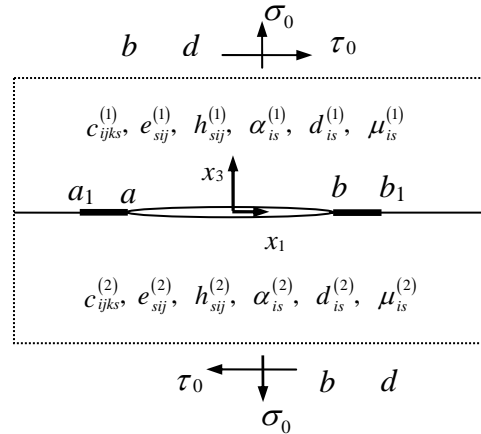


Figure 1. An interface crack with pre-fracture zones between two semi-infinite MEE planes

Assume that the MEE materials are poled in the x_3 –direction. As pointed out before [8], the displacement u_2 decouples in the (x_1, x_3) –plane from the displacement components u_1 , u_3 , electrical potential φ and magnetic potential ϕ . And in present study, our attention will be focused only on the generalized plane strain problem for the components u_1 , u_3 , φ and ϕ . Thus, for the considered magnetoelastically permeable interface crack, the continuity and boundary conditions at the interface can be written in the form

$$[[u_1], [u_3], [\varphi], [\phi]]^T = \mathbf{0}, [[\sigma_{31}], [\sigma_{33}], [D_3], [B_3]]^T = \mathbf{0}, x_1 \notin (a, b), \quad (1)$$

$$[\varphi] = 0, [D_3] = 0, [\phi] = 0, [B_3] = 0, x_1 \in (a, b), \quad (2)$$

$$\sigma_{33}^{(m)}(x_1, 0) \equiv p_1(x_1) = \begin{cases} \sigma' & x_1 \in [a_1, a], \\ \sigma, & x_1 \in [b, b_1], \\ 0, & x_1 \in [a, b], \end{cases} \quad \sigma_{31}^{(m)}(x_1, 0) \equiv p_2(x_1) = \begin{cases} \tau' & x_1 \in [a_1, a], \\ \tau, & x_1 \in [b, b_1], \\ 0, & x_1 \in [a, b], \end{cases} \quad (3)$$

where T denotes transposition, $[\Pi] = \Pi(x_1 + i0) - \Pi(x_1 - i0)$ ($\Pi = u_1, u_3, \text{etc.}$), and the values σ , τ , σ' and τ' are unknown to be determined.

In addition, as pointed out in Ref. [9], because the interlayer is usually much softer than the MEE materials, the interlayer yielding or damage will appear firstly. Thus, some law of interlayer material yielding or damage, for example, $f(\sigma, \tau, \sigma_1) = 0$ for the right pre-fracture zone and $f(\sigma', \tau', \sigma_1') = 0$ for the left pre-fracture zone, respectively, should be satisfied. For simplicity,

$\sigma_1 = \sigma_1' = 2\sigma_Y$ are assumed in present study [9].

Up till now, boundary conditions (i.e., Eqs. (1-3)) together with the known governing equations (see Ref. [8]) have formulated a plane strain problem of linear fracture mechanics for a crack $[a_1, b_1]$ between two half-planes, where the components σ , τ , σ' and τ' at the crack faces and the positions of point a_1 and b_1 are all unknown to be determined.

3. The magnetoelastostatic solution

From the early work [8], it is known that for the case of plane strain, the following expressions at

the interface hold true:

$$\mathbf{V}'(x_1) = [V'_1, V'_3, V'_4, V'_5]^T = [u'_1(x_1), u'_3(x_1), \varphi'(x_1), \phi'(x_1)]^T = \mathbf{W}^+(x_1) - \mathbf{W}^-(x_1),$$

$$\mathbf{t}^{(1)}(x_1, 0) = [\sigma_{31}^{(1)}, \sigma_{33}^{(1)}, D_3^{(1)}, B_3^{(1)}]^T = \mathbf{G}\mathbf{W}^+(x_1) - \bar{\mathbf{G}}\mathbf{W}^-(x_1),$$

where $\mathbf{W}(z) = [W_1(z), W_3(z), W_4(z), W_5(z)]^T$ is an introduced unknown vector function, and $\mathbf{W}^+(x_1) = \mathbf{W}(x_1 + i0)$, $\mathbf{W}^-(x_1) = \mathbf{W}(x_1 - i0)$; the matrix \mathbf{G} has been given in Ref. [8].

Considering that the crack is magnetoelectrically permeable, and that $\mathbf{t}^\infty = \mathbf{t}^{(1)}(x_1, 0)|_{x_1 \rightarrow \infty} = (\mathbf{G} - \bar{\mathbf{G}})\mathbf{W}(z)|_{z=x_1+i\epsilon_3 \rightarrow \infty}$ with $\mathbf{t}^\infty = \{\tau_0, \sigma_0, d_0, b_0\}^T$, we easily get

$$W_4 = \left\{ (\mathbf{G} - \bar{\mathbf{G}})^{-1} \mathbf{t}^\infty \right\}_3, \quad W_5 = \left\{ (\mathbf{G} - \bar{\mathbf{G}})^{-1} \mathbf{t}^\infty \right\}_4.$$

Taking into account that $W_4(z) = \text{const}$ and $W_5(z) = \text{const}$ and noting the structure of \mathbf{G} , we can further obtain

$$\sigma_{33}^{(1)}(x_1, 0) + i m_j \sigma_{31}^{(1)}(x_1, 0) = t_j [\Phi_j^+(x_1) + \gamma_j \Phi_j^-(x_1)], \quad (4)$$

$$[u'_1(x_1)] + i s_j [u'_3(x_1)] = \Phi_j^+(x_1) - \Phi_j^-(x_1). \quad (5)$$

where

$$\Phi_j(z) = \Omega_j(z) + \Phi_j^0, \quad \Phi_j^0 = \frac{2i(\mathcal{g}_{34}W_4 + \mathcal{g}_{35}W_5)}{t_j(1 + \gamma_j)}, \quad j = 1, 3,$$

$$\Omega_j(z) = W_1(z) + i s_j W_3(z), \quad \gamma_j = -\frac{\mathcal{g}_{31} + m_j \mathcal{g}_{11}}{t_j}, \quad t_j = \mathcal{g}_{31} - m_j \mathcal{g}_{11}, \quad j = 1, 3,$$

$$[u'_1] = W_1^+ - W_1^-, \quad m_{1,3} = m \sqrt{-\frac{\mathcal{g}_{31}\mathcal{g}_{33}}{\mathcal{g}_{11}\mathcal{g}_{13}}}, \quad s_{1,3} = -m_{1,3},$$

and \mathcal{g}_{ij} are the elements of \mathbf{G} .

Considering that $\Phi_j^+(x_1) = \Phi_j^-(x_1) = \Phi_j(x_1)$ for $x_1 \notin (a_1, b_1)$, it follows from Eq. (4) that

$$\Phi_j(z)|_{z \rightarrow \infty} = (\sigma_0 + i m_j \tau_0) / t_j (1 + \gamma_j). \quad (6)$$

Using Eq. (4) for $j = 1$ and the corresponding interface conditions (3) yields the following Hilbert problem

$$\Phi_1^+(x_1) + \gamma_1 \Phi_1^-(x_1) = P(x_1) / t_1, \quad x_1 \in (a_1, b_1), \quad (7)$$

where

$$P(x_1) = p_1(x_1) + i m_1 p_2(x_1).$$

The solution of Eq. (7) satisfying Eq. (6) can be expressed as

$$\Phi_1(z) = \frac{1}{2\pi i X(z)} \left[C_0 + C_1 z + \frac{1}{t_1} \int_{a_1}^{b_1} \frac{P(t) X^+(t)}{t - z} dt \right], \quad (8)$$

where

$$X(z) = (z - a_1)^{0.5 - i\epsilon} (z - b_1)^{0.5 + i\epsilon},$$

$$C_0 = -2\pi i \frac{\sigma_0 + i m_1 \tau_0}{t_1 (1 + \gamma_1)} \left(\frac{a_1 + b_1}{2} + i \epsilon l_1 \right), \quad C_1 = 2\pi i \frac{\sigma_0 + i m_1 \tau_0}{t_1 (1 + \gamma_1)}, \quad \epsilon = \ln \gamma_1 / 2\pi, \quad l_1 = b_1 - a_1.$$

Substituting Eq. (8) into Eq. (4) and noting that $\Phi_j^+(x_1) = \Phi_j^-(x_1) = \Phi_j(x_1)$ for $x_1 \notin (a_1, b_1)$, the following relation at the interface can be derived

$$\sigma_{33}^{(1)}(x_1, 0) + i m_1 \sigma_{31}^{(1)}(x_1, 0) = \frac{1}{2\pi i X(x_1)} \left\{ 2\pi i \left(x_1 - \frac{a_1 + b_1}{2} - i \varepsilon l_1 \right) (\sigma_0 + i m_1 \tau_0) + (1 + \gamma_1) \left[(\sigma' + i m_1 \tau') \int_{a_1}^a \frac{X^+(t)}{t - x_1} dt + (\sigma + i m_1 \tau) \int_b^{b_1} \frac{X^+(t)}{t - x_1} dt \right] \right\}. \quad (9)$$

Noting the finiteness of the stresses at the point a_1 and b_1 , we can further obtain the following system of linear algebraic equations

$$\begin{Bmatrix} \sigma' + i m_1 \tau' \\ \sigma + i m_1 \tau \end{Bmatrix} = \frac{\pi i l_1}{1 + \gamma_1} (\sigma_0 + i m_1 \tau_0) [\mathbf{N}]^{-1} \begin{Bmatrix} 1 + 2i \varepsilon \\ -(1 - 2i \varepsilon) \end{Bmatrix}, \quad (10)$$

where the components of matrix $\mathbf{N} = [N_{ij}] (i, j = 1, 2)$ have the following form

$$N_{11} = \int_{a_1}^a \left[\frac{(t - b_1)}{(t - a_1)} \right]^{0.5+i\varepsilon} dt, \quad N_{12} = \int_b^{b_1} \left[\frac{(t - b_1)}{(t - a_1)} \right]^{0.5+i\varepsilon} dt, \quad (11a)$$

$$N_{21} = \int_{a_1}^a \left[\frac{(t - a_1)}{(t - b_1)} \right]^{0.5-i\varepsilon} dt, \quad N_{22} = \int_b^{b_1} \left[\frac{(t - a_1)}{(t - b_1)} \right]^{0.5-i\varepsilon} dt. \quad (11b)$$

For the sake of simplicity to calculate, Eq. (11) can be further approximated (see Ref. [9]).

After substituting Eq. (10) into yielding conditions, a system of nonlinear equations is then derived as

$$\Psi_i(\Delta_a, \Delta_b, \sigma_0, \tau_0) = 0 \quad i = 1, 2, \quad (12)$$

where $\Delta_a = a - a_1$ and $\Delta_b = b_1 - b$ are the pre-fracture zone lengths.

Using Eq. (5), (7) and using (8), one arrives at the following equation on displacement jumps

$$\begin{aligned} [u_1(x_1)] + i s_1 [u_3(x_1)] &= \frac{1}{2\pi i \gamma_1 t_1} \left\{ 2\pi i (\sigma_0 + i m_1 \tau_0) (x_1 - a_1)^{0.5-i\varepsilon} (x_1 - b_1)^{0.5+i\varepsilon} + \right. \\ &\quad \left. (1 + \gamma_1) \left[(\sigma' + i m_1 \tau') J_1(x_1) + (\sigma + i m_1 \tau) J_2(x_1) \right] \right\} - \frac{1 - \gamma_1}{2\gamma_1 t_1} h(x_1), \end{aligned} \quad (13)$$

where

$$J_1(x_1) = \int_{a_1}^{x_1} \frac{1}{X(v)} \int_{a_1}^a \frac{X^+(t)}{t - v} dt dv, \quad J_2(x_1) = \int_{a_1}^{x_1} \frac{1}{X(v)} \int_b^{b_1} \frac{X^+(t)}{t - v} dt dv, \quad h(x_1) = \int_{a_1}^{x_1} P(t) dt.$$

The integral for $h_1(x_1)$ can be calculated analytically, and the integrals for $J_1(x_1)$ and $J_2(x_1)$ can be presented via hyper-geometric functions. As well known, for a real MEE bimaterial, ε is very small [6] and the influence of the oscillation on the value of $J_1(x_1)$ and $J_2(x_1)$ is negligibly small. Therefore by assuming $\varepsilon = 0$ in evaluating $J_1(x_1)$ and $J_2(x_1)$, one gets [9]

$$\begin{aligned} J_1(x_1) &\approx J_{10}(x) = \cos^{-1}(\alpha_1) \sqrt{(x - a_1)(b_1 - x)} + \frac{x - a}{2} H(a, b_1, x, a), \\ J_2(x_1) &\approx J_{20}(x) = \cos^{-1}(\alpha_1) \sqrt{(x - a_1)(b_1 - x)} - \frac{x - b}{2} H(a, b_1, x, b), \end{aligned}$$

where $\alpha_1 = (b_1 + a_1 - 2a)/l_1$, and $H(a, b, x, \xi)$ is a known function given in [9].

Thus, Eq. (13) can be rewritten as

$$\begin{aligned} [u_1(x_1)] + i s_1 [u_3(x_1)] &= (\sigma_0 + i m_1 \tau_0) (x_1 - a_1)^{0.5-i\varepsilon} (x_1 - b_1)^{0.5+i\varepsilon} / \gamma_1 t_1 + \\ &\quad (1 + \gamma_1) \left[(\sigma' + i m_1 \tau') J_{10}(x_1) + (\sigma + i m_1 \tau) J_{20}(x_1) \right] / 2\pi i \gamma_1 t_1 - h(x_1) (1 - \gamma_1) / 2\gamma_1 t_1. \end{aligned} \quad (14)$$

Crack opening displacements (COD) at the initial crack tips are defined as follows

$$\delta_1^a = [u_1(a)], \quad \delta_3^a = [u_3(a)], \quad \delta_1^b = [u_1(b)], \quad \delta_3^b = [u_3(b)]. \quad (15)$$

After substituting $x_1 = a, b$, respectively, into the expressions of $[u_1(x_1)]$, $[u_3(x_1)]$ and the COD in Eq. (15) will be then acquired as well. In addition, carrying out a similar derivation to the one given in [9], the expressions for the electrical displacement and magnetic induction at different segments of the interface can be easily obtained (omitted here).

It is remarked that both the electrical displacement $D_3^{(1)}(x_1, 0)$ and magnetic induction $B_3^{(1)}(x_1, 0)$ are not singular as well at either the initial crack tips or the points a_1 and b_1 . Thus, the proposed model removes singularities in all components of the magnetoelectromechanical field. On the other hand, it should be pointed out that both the electrical displacement and magnetic induction in the pre-fracture zone are not only directly related to the material parameters of MEE bimaterial and the applied tension load, but also related to $[u_1'(x_1)]$ and the normal stress in the pre-fracture zone, and that the electrical displacement in the pre-fracture zone depends on the applied electrical load, and magnetic induction on magnetic load. However, both the normal and shear stresses in the pre-fracture zone are independent of the applied magnetoelectrical load.

4. Simplified case of symmetrical loads

For the case of symmetrical loads, i.e., $\tau_0 \equiv 0$, placing the apex of the coordinate system in the middle point of the crack, one has $a = -b$, $a_1 = -b_1$, $\tau' = -\tau$, $\sigma' = \sigma$. In Eq. (10), only one of the equations is necessary, which can be expressed as

$$(\sigma - im_1\tau)N_{21}^{sym} + (\sigma + im_1\tau)N_{22}^{sym} = -\frac{2\pi i b_1}{1 + \gamma_1} \sigma_0 (1 - 2i\varepsilon). \quad (16)$$

where

$$N_{21}^{sym} = \frac{1}{1.5 - i\varepsilon} (-2b_1)^{-0.5+i\varepsilon} (b_1 - b)^{1.5-i\varepsilon}, \quad N_{22}^{sym} = -\frac{1}{0.5 + i\varepsilon} (2b_1)^{0.5-i\varepsilon} (b - b_1)^{0.5+i\varepsilon}.$$

Extracting the real and imaginary parts of Eq. (16), we arrive at the system of linear algebraic equations with respect to σ and τ . The solution of the obtained system can be expressed as

$$\sigma = rm_1\sigma_0(2\varepsilon a_{22} - a_{12}), \quad \tau = r\sigma_0(2\varepsilon a_{21} + a_{11}), \quad (17)$$

where the expressions for r and a_{ij} ($i, j = 1, 2$) are the same as those given in [9]. It is worth noting that the values of r , a_{ij} and consequently σ and τ all depend on the pre-fracture zone length $g = b/b_1$.

Substituting Eq. (17) into the second equation of Eq. (12) and taking into account that $\Delta_a = \Delta_b$ in the considered case, one arrives at a transcendental equation with respect to g as follows

$$\left[m_1(2\varepsilon a_{22} - a_{12}) - \frac{\sigma_1}{r\sigma_0} \right]^2 + 4(2\varepsilon a_{21} + a_{11})^2 = \frac{4}{3r^2} \left(\frac{\sigma_Y}{\sigma_0} \right)^2,$$

where the Mises yielding condition $f(\sigma, \tau, \sigma_1) \equiv (\sigma - \sigma_1)^2 + 4\tau^2 - \frac{4}{3}\sigma_Y^2 = 0$ and $\sigma_1 = 2\sigma_Y$ are used [9].

From Eq. (14), the displacement jumps for $x_1 \in (-b_1, b_1)$ can be then obtained as

$$\begin{aligned} [u_1(x_1, 0)] + i s_1 [u_3(x_1, 0)] &\approx \sigma_0 (x_1 + b_1)^{0.5-i\varepsilon} (x_1 - b_1)^{0.5+i\varepsilon} / \gamma_1 t_1 \\ &+ (1 + \gamma_1) [(\sigma - im_1\tau)J_{10}^{sym}(x_1) + (\sigma + im_1\tau)J_{20}^{sym}(x_1)] / 2\pi i \gamma_1 t_1 - h(x_1)(1 - \gamma_1) / 2\gamma_1 t_1, \end{aligned}$$

where $J_{i0}^{sym}(x_1) = J_{i0}(x_1)$ ($i = 1, 2$) with $a = -b$, $a_1 = -b_1$. And the electrical displacement and magnetic induction can be expressed as

$$D_3^{(1)}(x_1, 0) = -\frac{\vartheta_0}{\vartheta_{43}} \frac{\vartheta_6^1}{\vartheta_{33}} \sigma_0 + d_0 + \begin{cases} \eta_1 [u'_1(x_1)] + \frac{\vartheta_0}{\vartheta_{43}} \frac{\vartheta_6^1}{\vartheta_{33}} \sigma, & x_1 \in (a_1, a) \cup (b, b_1), \\ \eta_1 [u'_1(x_1)], & x_1 \in (a, b), \\ \frac{\vartheta_0}{\vartheta_{43}} \frac{\vartheta_6^1}{\vartheta_{33}} \sigma_{33}^{(1)}(x_1, 0), & x_1 \notin (a_1, b_1), \end{cases}$$

$$B_3^{(1)}(x_1, 0) = -\frac{\vartheta_0}{\vartheta_{33}} \frac{\vartheta_6^1}{\vartheta_{33}} \sigma_0 + b_0 + \begin{cases} \eta_2 [u'_1(x_1)] + \frac{\vartheta_0}{\vartheta_{33}} \frac{\vartheta_6^1}{\vartheta_{33}} \sigma, & x_1 \in (a_1, a) \cup (b, b_1), \\ \eta_2 [u'_1(x_1)], & x_1 \in (a, b), \\ \frac{\vartheta_0}{\vartheta_{33}} \frac{\vartheta_6^1}{\vartheta_{33}} \sigma_{33}^{(1)}(x_1, 0), & x_1 \notin (a_1, b_1), \end{cases}$$

where $\eta_1 = \frac{\vartheta_0}{\vartheta_{41}} - \frac{\vartheta_0}{\vartheta_{43}} \frac{\vartheta_{31}}{\vartheta_{33}}$, $\eta_2 = \frac{\vartheta_0}{\vartheta_{31}} - \frac{\vartheta_0}{\vartheta_{33}} \frac{\vartheta_{31}}{\vartheta_{33}}$.

5. Case of equivalent properties of the upper and lower bimaterial components

In this case, $\gamma_1 = 1$, $\varepsilon = 0$ hold true and Eq. (9) takes the form

$$\sigma_{33}^{(1)}(x_1, 0) + im_1 \sigma_{31}^{(1)}(x_1, 0) = \frac{\sigma_0 + im_1 \tau_0}{X_0(x_1)} \left(x_1 - \frac{a_1 + b_1}{2} \right) + \frac{1}{\pi i X_0(x_1)} \left[(\sigma' + im_1 \tau') \int_{a_1}^a \frac{X_0^+(t)}{t - x_1} dt + (\sigma + im_1 \tau) \int_b^{b_1} \frac{X_0^+(t)}{t - x_1} dt \right], \quad x_1 \notin (a_1, b_1), \quad (18)$$

where $X_0(z) = \sqrt{(z - a_1)(z - b_1)}$.

Using Eq. (10), the pre-fracture zone stresses can be calculated by the following formula

$$\begin{Bmatrix} \sigma' + im_1 \tau' \\ \sigma + im_1 \tau \end{Bmatrix} = \frac{\pi i l_1}{2} (\sigma_0 + im_1 \tau_0) \mathbf{N}^{-1} \begin{Bmatrix} 1 \\ -1 \end{Bmatrix}.$$

Components of the matrix \mathbf{N} can be written exactly as

$$N_{11} = i \frac{l_1}{2} \left[\sqrt{1 - \alpha_1^2} + \cos^{-1}(\alpha_1) \right], \quad N_{12} = i \frac{l_1}{2} \left[\cos^{-1}(\alpha_2) - \sqrt{1 - \alpha_2^2} \right],$$

$$N_{21} = i \frac{l_1}{2} \left[\sqrt{1 - \alpha_1^2} - \cos^{-1}(\alpha_1) \right], \quad N_{22} = -i \frac{l_1}{2} \left[\cos^{-1}(\alpha_2) + \sqrt{1 - \alpha_2^2} \right],$$

where $\alpha_2 = (2b - b_1 - a_1)/l_1$.

For this case, the expression for the displacement jump has the following form

$$[u_1(x_1, 0)] + is_1 [u_3(x_1, 0)] = (\sigma_0 + im_1 \tau_0) \sqrt{(x_1 - a_1)(x_1 - b_1)} / t_1 + [(\sigma' + im_1 \tau') J_{10}(x_1) + (\sigma + im_1 \tau) J_{20}(x_1)] / \pi i t_1, \quad x_1 \in (a_1, b_1). \quad (19)$$

And δ_1^a , δ_3^a , δ_1^b and δ_3^b can then be obtained easily.

In this case of homogeneous material with symmetrical loading, one has $\tau = \tau' = 0$ and $\sigma' = \sigma$. In the coordinate system with apex in the middle of the crack, $\sigma_{31}^{(1)}(x_1, 0) = 0$, $a = -b$, $a_1 = -b_1$ hold true. And only one equation of Dugdale -type $\sigma = \sigma_c$ [10] can be considered. In addition, according to the von Mises yielding condition given before, σ_c is related to the material parameters of interlayer, which can be taken as $2(1 + 1/\sqrt{3})\sigma_Y$. Furthermore, for this case $\alpha_2 = \alpha_1 = b/b_1$ and Eq. (18) can be reduced as

$$\sigma_{33}^{(1)}(x_1, 0) = \frac{1}{\sqrt{x_1^2 - b_1^2}} \left\{ \sigma_0 x_1 + \frac{\sigma_c}{\pi i} \left(\int_{-b_1}^{-b} + \int_b^{b_1} \right) \frac{\sqrt{t^2 - b_1^2}}{t - x_1} dt \right\}, \quad x_1 \notin (a_1, b_1). \quad (20)$$

By setting the expression in the brackets to zero, one gets the following equation

$$\frac{b}{b_1} = \cos \frac{\pi \sigma_0}{2\sigma_c}. \quad (21)$$

Thus, the pre-fracture zone length can easily be determined from Eq. (21). By the way, it is easily known that for internal crack problem of identical MEE material, although the length of pre-fracture zone depends on σ_0 , σ in the pre-fracture zone is independent of it.

It is worth noting that after evaluating the integrals in Eq. (20) and using (21), one gets [9]

$$\sigma_{33}^{(1)}(x_1, 0) = \sigma_c + \frac{\sigma_c}{\pi} \left[\sin^{-1} \frac{b_1^2 - x_1 b}{b_1(x_1 - b)} - \sin^{-1} \frac{b_1^2 + x_1 b}{b_1(x_1 + b)} \right], \quad x_1 \notin (a_1, b_1).$$

Considering only imaginary part of Eq. (19) and noting $[u_1(x_1)] = 0$ and Eq. (21), we have

$$[u_3(x_1)] = \frac{\sigma_c}{2\pi t_1 s_1} [(x_1 - b)H(-b_1, b_1, x_1, b) - (x_1 + b)H(-b_1, b_1, x_1, -b)]. \quad (22)$$

The COD at the initial crack tip can be obtained for $x_1 = b$ and can be written in the form

$$\delta_3^b = -\frac{2b\sigma_c}{\pi t_1 s_1} \ln \left(\cos \frac{\pi \sigma_0}{2\sigma_c} \right). \quad (23)$$

It is important to note that for the case of isotropic upper and lower bimaterial components with $t_1 = 2\mu/(1+\kappa)$, $s_1 = 1$ [11], Eqs. (22) and (23) formally coincide with the associated equation of Panasyuk [12], and that the expressions for the electrical displacement and magnetic induction at the interface can be expressed in a simple form (omitted here).

6. Numerical results and discussion

In this section, for simplicity, numerical calculations only for the case of symmetric loads are carried out. As an example, material combination A/B of material A (upper material) and B (lower one) is mainly investigated. The material constants of them for material A with volume fraction $v_f=0.3$ and for material B with volume fraction $v_f=0.5$ are given by Sih and Song [13]. The interface layer was assumed to be elastic-perfectly plastic material with yield stress $\sigma_Y = 220\text{MPa}$ [9]. In addition, loading combination parameters $\lambda_D = d_0 e_{33}^{(1)}/(\sigma_Y \alpha_{33}^{(1)})$ and $\lambda_B = b_0 h_{33}^{(1)}/(\sigma_Y \mu_{33}^{(1)})$ are introduced to reflect the applied electrical and magnetic loads, respectively.

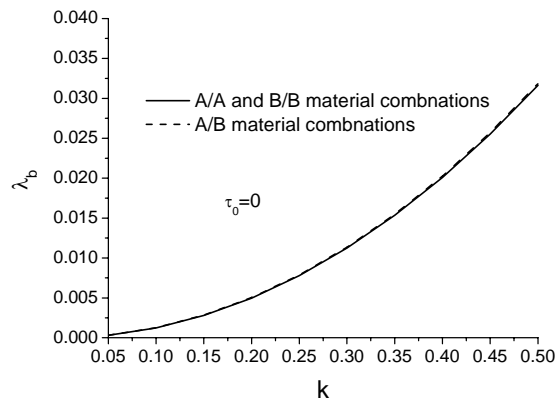


Figure 2. Relative pre-fracture zone lengths versus the applied tension load

The numerical results for the relative pre-fracture zone lengths, stresses in pre-fracture zones and

the CODs at the initial crack tips with respect to the normalized applied normal load for different material combinations are presented in Figures 2-6, where $k = \sigma_0/\sigma_Y$, $l = (b-a)/2$, $\lambda_b = \Delta_b/l$ and $\lambda_D = \lambda_B = 0$. And if no special explanation is given, all the curves in these figures consider only A/B combination. It is remarked that because of the symmetry, only the corresponding numerical results for the right pre-fracture zone are plotted.

Figure 2 shows that the pre-fracture zone length of all current material combinations increases with the increasing of applied tension load and it is interesting to note that the pre-fracture zone length of A/B material combination is only slightly larger than that of A/A or B/B material combinations. Besides, the values of pre-fracture zone length are much smaller than the crack length, even for a relatively large external load. Figure 2 also indicates that for the internal crack problem of identical MEE material, the pre-fracture zone length is independent of the material properties of MEE material.

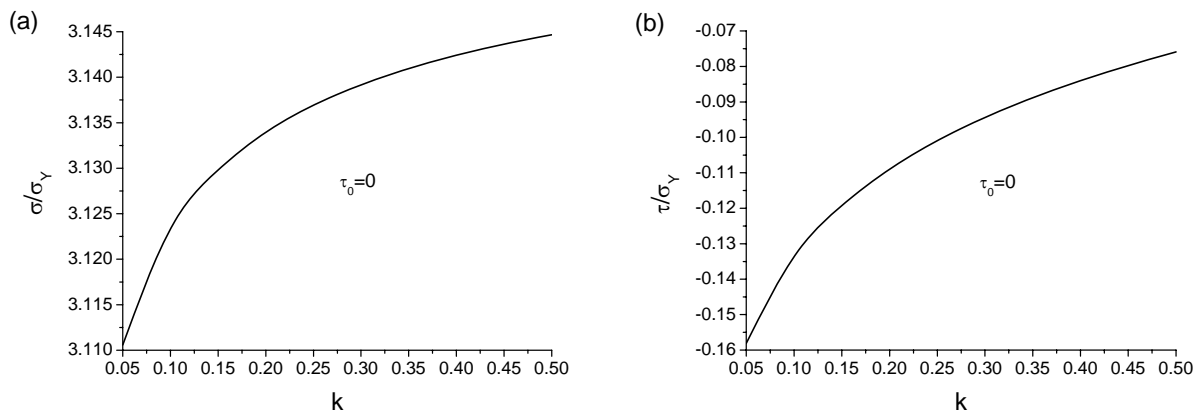


Figure 3. Normalized (a) normal stress and (b) shear stress in the pre-fracture zone versus the applied tension load

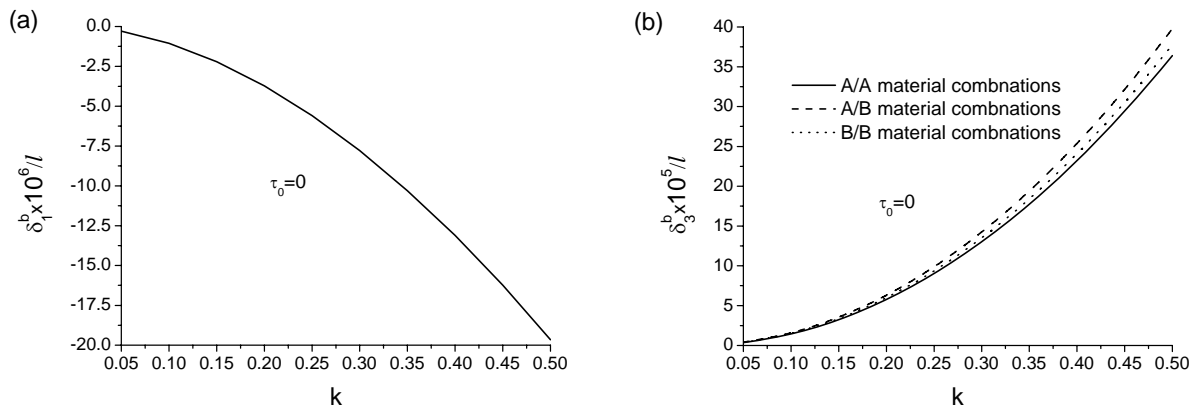


Figure 4. Normalized CODs at the initial crack tip versus the applied tension load

From Figure 3, it can be seen that for A/B material combination, the normal stress in the pre-fracture zones increases with the increasing of normalized normal load k , while the magnitude of shear stress decreases with the increasing of normalized tension load. The similar phenomena have been observed by Loboda et al. [9] for interface crack problem of piezoelectric bimaterial.

As shown in Figure 4, with the increasing of normalized normal load, although δ_1^b is negative, the

magnitude of δ_1^b at initial crack tips increases for A/B combination, and δ_3^b increases for A/B, A/A and B/B combinations. It should be pointed out that, as expected, for the considered loading cases, δ_3^b is much larger than δ_1^b . In addition, it is interesting to note from Figure 4b that for A/B combination, δ_3^b is slightly larger than that of both A/A and B/B combinations, which is a novel phenomenon different to the one observed in [9] for piezoelectric bimaterial problem.

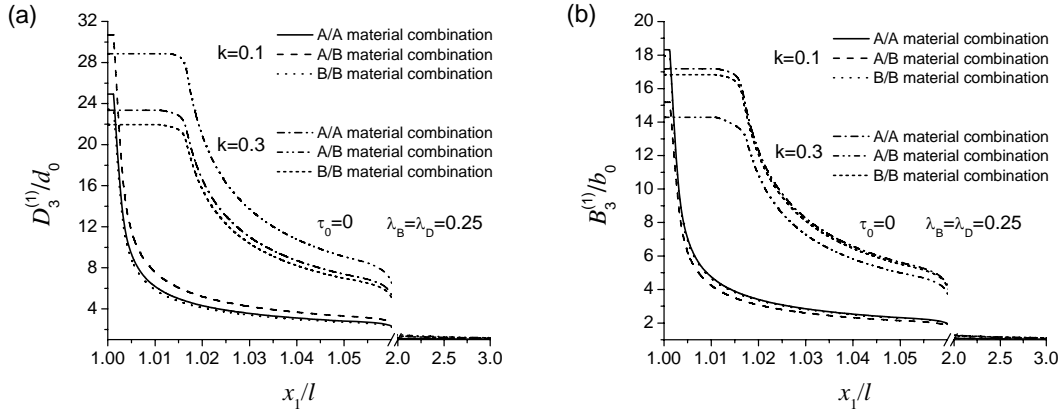


Figure 5. Normalized (a) electrical displacement and (b) magnetic induction along the interface under different tension loads

In Figure 5, the distributions of normalized electrical displacement $D_3^{(1)}(x_1,0)/d_0$ and normalized magnetic induction $B_3^{(1)}(x_1,0)/b_0$ along the crack face are presented, where $\lambda_D = \lambda_B = 0.25$. For $k = \sigma_0/\sigma_Y = 0.1$ and 0.3 , the pre-fracture zone lengths can be easily determined by Eq. (21). They are, respectively, $\lambda_a = \lambda_b = 0.00124$ and 0.01124 , which, in fact, are the same as those given by Loboda et.al [9] for piezoelectric crack problem with pre-fracture zone. As shown in Figure 5, on one hand, the applied tension loads have significant effects on both the electrical displacement and magnetic induction in the pre-fracture zone. On the other hand, for a definite tension load, both the electrical displacement and magnetic induction in the pre-fracture zone are almost unchanged. In addition, with the increasing of x_1/l , both the electrical displacement and magnetic induction decrease rapidly, and as expected, the values of $D_3^{(1)}(x_1,0)/d_0$ and $B_3^{(1)}(x_1,0)/b_0$ finally approach to 1.

6. Conclusion

A plane strain problem for two MEE half-planes adhered by means of a very thin isotropic interlayer has been considered. A novel interface crack model, i.e., an interface crack with both open part and pre-fracture zone is put forward. The crack surfaces are assumed to be magnetoelectrically permeable. The problem is firstly reduced to a Hilbert problem on the unknown normal stress and shear stress in the pre-fracture zones, which can be solved exactly. By introducing Mises yielding conditions on interface layer, a system of nonlinear equations is established to determine pre-fracture zone lengths. Finally, the corresponding results for both cases of symmetric load and equivalent properties of the upper and lower bimaterial components are further obtained. From the theoretical and numerical results, the following conclusions can be drawn:

- For the suggested model, all mechanical, electrical and magnetic characteristics are limited in the near-crack tip region, i.e., all singularities connected with the model are eliminated.

- For the magnetoelectrically permeable interface crack with pre-fracture zones, δ_3^b plays a very important role in the fracture analysis of the interface crack because it is much larger than δ_1^b . And in general, increasing tension loads will cause crack growth and propagation.
- For the internal crack problem of identical MEE material under symmetrical load, the pre-fracture zone lengths are independent of material properties, and the normal stress in the pre-fracture zone is independent of applied tension load.

Acknowledgement

The supports from the National Natural Science Foundation of China (Grant Nos. 10772123 and 11072160) are acknowledged.

References

- [1] C.F. Gao, H. Kessler, H. Balke, Crack problems in magneto-electroelastic solids. Part I: Exact solution of a crack. *Int J Eng Sci* 41(2003) 969-981.
- [2] G.C. Sih, R. Jones, Z.F. Song, Piezomagnetic and piezoelectric poling effects on mode I and II crack initiation behavior of magneto-electroelastic materials. *Theor Appl Fract Mech* 40(2003) 161-186.
- [3] W.Y. Tian, U. Gabbert, Macrocrack-microcrack interaction problem in magneto-electroelastic solids. *Mech Mater* 37(2005) 565-592.
- [4] X.H. Chen, Energy release rate and path-independent integral in dynamic fracture of magneto-electro-thermo-elastic solids. *Int J Solids Struct* 46(2009) 2706-2711.
- [5] X.C. Zhong, F. Liu, X.F. Li, Transient response of a magneto-electroelastic solid with two collinear dielectric cracks under impacts. *Int J Solids Struct* 46(2009) 2950-2958.
- [6] R. Li, G.A. Kardomateas, The mixed mode I and II interface crack in piezoelectromagneto-elastic anisotropic bimetals. *ASME J Appl Mech* 74(2007) 614-627.
- [7] K.P. Herrmann, V.V. Loboda, T.V. Khodanen, An interface crack with contact zones in a piezoelectric/piezomagnetic biomaterial. *Arch Appl Mech* 80(2010) 651-670.
- [8] W.J. Feng, P. Ma, E. Pan, J.X. Liu, A magnetically impermeable and electrically permeable interface crack with a contact zone in a magneto-electroelastic bimaterial under concentrated magneto-electromechanical loads on the crack faces. *Sci China: Physics, Mechanics and Astronomy* 54(2011) 1666-1679.
- [9] V. Loboda, Y. Lapusta, A. Sheveleva, Electro-mechanical pre-fracture zones for an electrically permeable interface crack in a piezoelectric bimaterial. *Int J Solids Struct* 44(2007) 5538-5553.
- [10] D.S. Dugdale, Yielding of steel sheets containing slits. *J Mech Phys Solids* 8(1960) 100–108.
- [11] K.P. Herrmann, V.V. Loboda, I.V. Kharun, Interface crack with a contact zone in an isotropic bimaterial under thermomechanical loading. *Theor Appl Fract Mech* 42(2004) 335–348.
- [12] V.V. Panasyuk, Limiting equilibrium of brittle solids with fracture [in Russian], Naukova, 1968, Dumka Publishers, Kiev, translation in English: Detroit. Michigan Inform. Serv, 197, pp 284.
- [13] G.C. Sih, Z.F. Song, Magnetic and electric poling effects associated with crack growth in BaTiO₃-CoFe₂O₄ composite. *Theor Appl Fract Mech* 39(2003) 209–227.